
Well-Log-Based Analysis of Pore Pressure and Minimum Effective Stress (Fracture Gradient) in the Penobscot B-41 Well, Offshore Nova Scotia

Henri Jeni Tua Baringin Sitohang^{1*}

¹Program Magister Ilmu Fisika, Universitas Indonesia

e-mail: henri_jeni@yahoo.com

Article Info

Article history:

Received : August 24th, 2025

Revised : October 19th, 2025

Accepted : October 30th, 2025

Available online : October 31st, 2025

<https://doi.org/10.33541/edumatsains.v10i2.7306>

Abstract

This study analyzes pore pressure (P_p) and minimum effective stress (fracture gradient) in the Penobscot Offshore Field using well log data from wells Penobscot B-41. The Eaton and Bowers methods were applied to estimate pore pressure and minimum effective stress (fracture gradient), while vertical stress (σ_v) and minimum horizontal stress (σ_{hmin}) were calculated from density data. The results indicate the presence of a top overpressure zone beginning at approximately 8,376 ftTVD, marked by a significant deviation from the normal compaction trend. A reversal depth is also identified around 9,000-9,200 ftTVD, indicating a shift in the overpressure mechanism from normal compaction to unloading. Pore pressure values derived from both Eaton and Bowers methods show overall consistency, although Bowers tends to yield more conservative estimates in the deeper sections. Unloading is particularly evident in the deeper interval of well Penobscot B-41, where elevated ΔDT values are observed without corresponding low density, suggesting stress release caused by fracturing or fluid migration. Effective stress ($\sigma_v - P_p$) calculations reveal high-risk zones for fracturing at depths greater than 9,500 ftTVD, which should be carefully addressed in mud weight design. Overall, the integration of Eaton and Bowers methods with effective stress evaluation successfully characterizes the geopressed system of the Penobscot Field. These findings provide an essential basis for drilling risk mitigation and casing design optimization.

Keywords: pore pressure, minimum effective stress, Eaton's method, Bowers model, Penobscot field.

1. Introduction

The estimation of pore pressure and minimum effective stress (commonly referred to as fracture gradient) represents a fundamental aspect of oil and gas well drilling operations. Inaccuracies in predicting these two parameters may lead to severe consequences such as kicks, blowouts, and lost circulation, which directly affect operational safety, costs, and well integrity. Excessive pore pressure can result in drilling mud being unable to contain formation fluid influx, while miscalculation of the fracture gradient may induce uncontrolled fracturing of the formation, causing mud losses into permeable zones. Therefore, the accuracy of subsurface pressure prediction is not only a technical requirement but also a critical element of risk management in ensuring both operational safety and the economic viability of drilling projects.

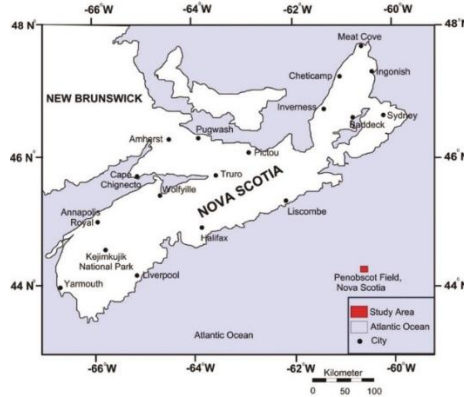
A thorough assessment of pore pressure and fracture gradient distribution is essential for designing an optimal mud weight window. The mud weight window defines the safe drilling margin, constrained by pore pressure on the lower bound and fracture gradient on the upper bound. A narrow drilling window demands highly accurate geomechanical modeling, as even minor errors may trigger influx or mud losses. Previous studies have demonstrated that well-log-based approaches provide high-resolution insights for identifying abnormal pressure anomalies, thereby offering a reliable basis for mitigating operational risks (Eaton, 1975; Bowers, 1995; Swarbrick & Osborne, 1998). Accordingly, pore pressure and minimum effective stress modeling serves as a strategic step in ensuring safe and successful drilling operations.

In the context of the Penobscot Offshore Field, accurate characterization of pore pressure and fracture gradient is particularly important since this field exhibits evidence of overpressure and unloading mechanisms at specific depths. The integration of empirical methods such as Eaton's approach and the Bowers velocity model, combined with normal compaction trend (NCT) analysis on shale intervals, enables a more comprehensive representation of the geopressure system within the basin. The outcomes of this study are expected not only to enhance safe drilling design but also to contribute to the broader scientific understanding of overpressure development mechanisms in the passive margin of the Northwest Atlantic.

The Penobscot Field is located offshore Nova Scotia, in eastern Canada, and forms part of the Northwest Atlantic passive margin (Figure 1).

Figure 1.

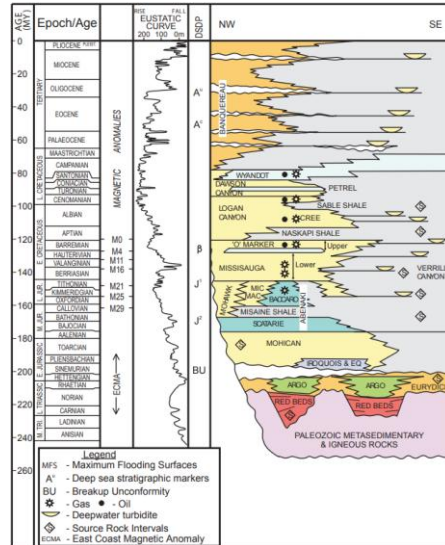
Location map of the Penobscot Field within the Scotian Basin, offshore Nova Scotia, Canada.



The map illustrates the tectono-stratigraphic framework of the basin as part of the Northwest Atlantic passive margin.

The Scotian Basin developed during the Early to Middle Jurassic in response to the rifting and subsequent breakup of the supercontinent Pangea, which initiated the opening of the Atlantic Ocean (Wade & MacLean, 1990). This tectonic evolution produced a series of grabens and half-grabens that were subsequently infilled by thick successions of clastic sediments throughout the Mesozoic. The stratigraphic record of the basin reflects repeated cycles of transgression and regression, with clastic deposition dominating much of the sedimentary fill. Within this stratigraphic framework, the Missisauga Formation represents the principal reservoir unit, consisting predominantly of turbidite sandstones (Figure 2).

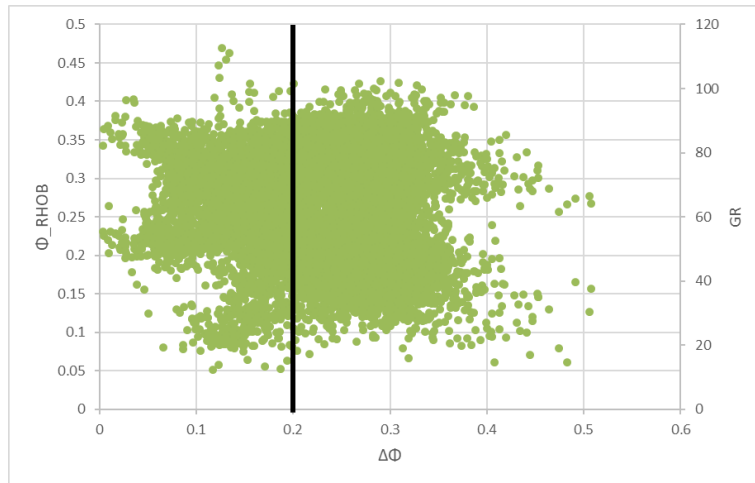
Figure 2.
Regional stratigraphic column of the Scotian Basin, offshore Nova Scotia, Canada.



The succession highlights the main petroleum system elements, including the Missisauqua Formation as the primary sandstone reservoir, the Verrill Canyon Formation as both source and seal, and the carbonate interval of the Abenaki Formation as an additional source rock.

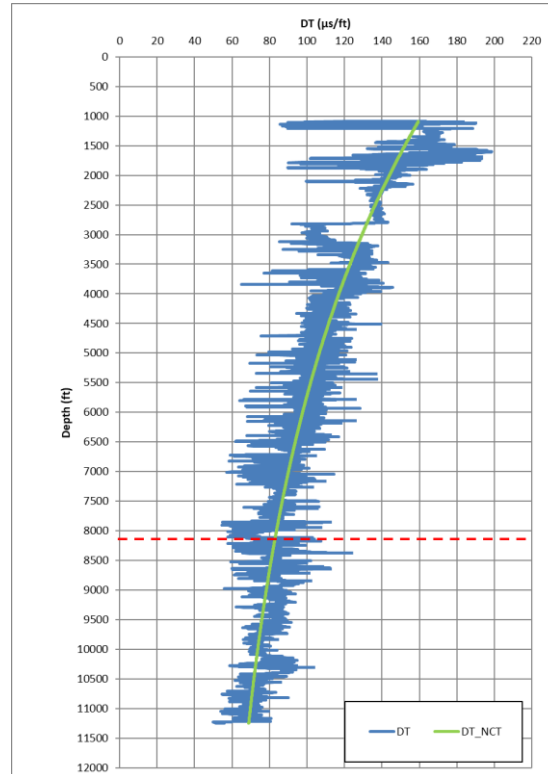
Figure 3.

Cross-plot of density-derived porosity, neutron–density porosity difference ($\Delta\Phi$), and gamma ray (GR) values used for shale identification in the shale-picking process.



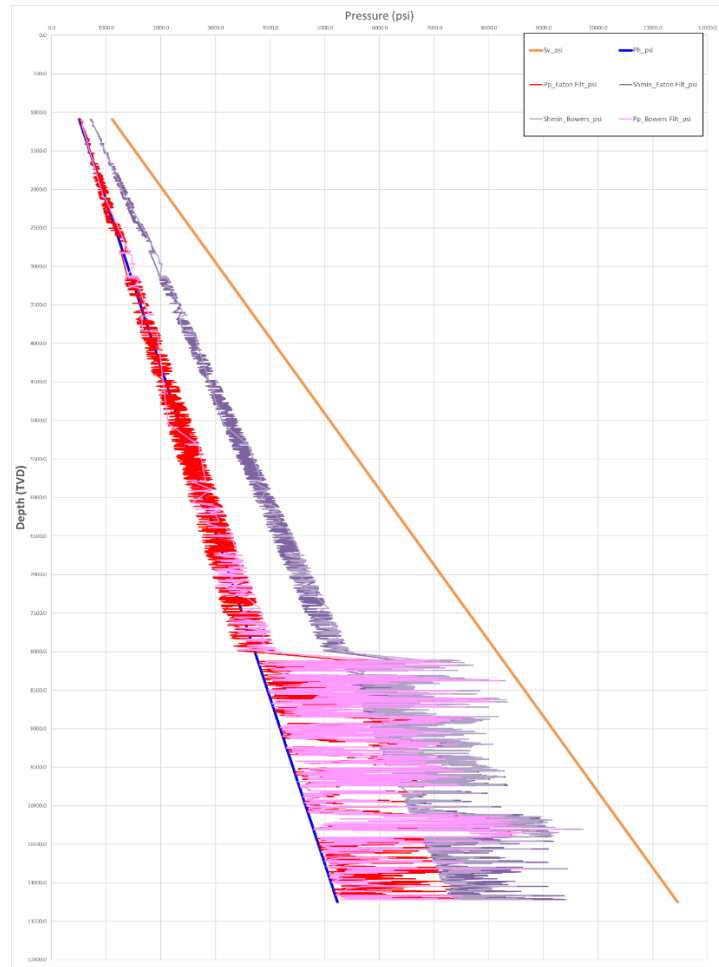
The combined parameters provide a robust criterion for defining pure shale intervals that form the basis for the Normal Compaction Trend (NCT).

Figure 4.
Cross-plot of the sonic NCT in the Penobscot B-41 well.



Deviations between measured sonic transit time (Δt) and the NCT become evident at depths of approximately 8,300–8,500 ft TVD (indicated by the dashed red line), where Δt values are higher (slower velocity) than predicted by the compaction trend, marking the onset of overpressure.

Figure 5.
Formation pressure cross-plot for the Penobscot B-41 well.



Both Eaton and Bowers pore pressure models consistently indicate the presence of overpressure beginning at ~8,376 ft TVD, reflecting a transition from normal compaction to unloading as the dominant overpressure mechanism.

Overlying the reservoir, the Verrill Canyon Formation comprises organic-rich marine shales that act as both a primary source rock and an effective regional seal. Additionally, the Abenaki Formation, composed of carbonate facies, contributes further hydrocarbon potential as a supplementary source rock (Jansa & Wade, 1975; Kidston et al., 2002). Together, these formations establish the essential elements of a working petroleum system in the Scotian Basin. Hydrocarbon generation and expulsion were driven by deep burial and progressive compaction from the Late

Jurassic through the Cretaceous, resulting in the accumulation of oil and gas within structural and stratigraphic traps. The petroleum system of the Penobscot Field is controlled by the interplay of source, reservoir, and seal rocks. The organic-rich shales of the Verrill Canyon and Abenaki formations provide sufficient hydrocarbon charge, while the Missisauga turbidite sandstones serve as high-quality reservoirs, and the overlying Verrill Canyon marine shales function as an effective seal. The principal structural configurations include: (i) normal faults related to extensional tectonics of the passive margin; (ii) rollover anticlines formed through the reactivation of normal faults; and (iii) combination structural-stratigraphic traps, where turbidite sandstones are confined laterally and vertically by shale intervals of the Verrill Canyon Formation. Unlike tectonically active margins, the Scotian Basin experienced limited compressional deformation during the Neogene–Recent, resulting in preservation of extensional structures typical of passive continental margins.

From a geomechanical perspective, the dominant mechanism of overpressure generation in the basin is associated with undercompaction of fine-grained clastic sediments deposited under high sedimentation rates. However, well-log evidence from the Penobscot B-41 indicates the presence of unloading phenomena at greater depths, manifested as sonic velocity reversals not accompanied by significant density reductions. Such anomalies are interpreted to reflect secondary processes, including fluid release or fracture development, which modify the pressure regime beyond simple disequilibrium compaction (Swarbrick & Osborne, 1998). These insights underscore the importance of integrating geological, stratigraphic, and geomechanical perspectives in developing a comprehensive understanding of the basin's petroleum system and pressure evolution.

2. Methods

This research is focused on the Penobscot Offshore Field located in the Scotian Basin, Nova Scotia, which has been made available as an open-source dataset for academic and applied geoscientific studies. The analysis was conducted using well-log data from well Penobscot B-41, chosen for its comprehensive logging suite that enables pore pressure and stress evaluation.

The methodology employed in this study consisted of several key stages. First, a Normal Compaction Trend (NCT) was established using intervals of pure shale identified through shale-picking procedures. Shale intervals are critical for compaction analysis since their acoustic and density responses reflect burial stress without significant influence from lithological heterogeneity. Deviations from the NCT were then interpreted as indicators of overpressure development. Pore pressure (P_p) was subsequently calculated using two widely recognized velocity-based models: the Eaton method (1975), which provides a conservative estimate of pore pressure under conditions of undercompaction, and the Bowers model (1995), which is capable of capturing unloading phenomena at greater depths. This dual-model approach ensures a more reliable representation of the pore pressure regime by addressing different mechanisms of overpressure generation.

In addition, vertical stress (σ_v) was computed by integrating the density log over depth, thereby providing an estimate of the total overburden pressure. The minimum horizontal stress

(σ_{hmin}), representing the fracture gradient, was derived using both elasticity-based equations and empirical correlations, with Poisson’s ratio values calibrated for shale lithologies. This integration of petrophysical and geomechanical models allowed for the determination of the mud weight window, which is essential for well design and safe drilling operations.

Well Data

The dataset used in this study was obtained from well Penobscot B-41, which includes Gamma Ray (GR) logs, Resistivity logs, Density (RHOB) logs, and Sonic (DT) logs. These logs provide the fundamental parameters required to define shale intervals, construct compaction trends, and apply velocity-based pore pressure prediction methods. The combination of these datasets enabled a comprehensive analysis of subsurface pressure conditions and geomechanical properties within the Penobscot Field.

Shale Picking as the Basis for the Normal Compaction Trend (NCT)

The selection of pure shale intervals (shale picking) is a critical step in establishing the Normal Compaction Trend (NCT), which serves as the baseline for pore pressure estimation. The objective of this process is to identify log responses that accurately represent normal compaction conditions, free from the influence of non-shale lithologies or porosity anomalies. Appropriately selected shale intervals ensure that pore pressure predictions are both stable and reliable (Horsrud, 2001; Dutta, 2002).

In this study, shale picking was conducted using a quantitative approach that integrates multiple indicators to enhance accuracy:

a. Density-Derived Porosity (Φ_D)

Porosity was calculated from the density log (RHOB) using an assumed matrix density (ρ_{matrix}) of 2.65 g/cc (quartz/sandstone) and a fluid density (ρ_f) of 1.03 g/cc (formation water). The equation is expressed as:

$$\Phi_D = \frac{\{\rho_{matrix}\} - \rho_{\{b\}}}{\{\rho_{matrix}\} - \rho_{\{f\}}}$$

.....(eq 1)

Where:

- Φ_D = Density-derived porosity
- $\rho_{\{matrix\}}$ = Matrix density (2.65 g/cc)
- $\rho_{\{b\}}$ = Bulk density from the RHOB log (RHOB)
- $\rho_{\{f\}}$ = Formation water density (1.03 g/cc)

In general, shale intervals display relatively higher density-derived porosity compared to more consolidated sandstone lithologies (Athy, 1930).

b. $\Delta\Phi$ (Neutron–Density Porosity Cross-plot)

$\Delta\Phi$ was calculated as the difference between neutron porosity (NPHI) and density-derived porosity (Φ_D). Clay-rich shales typically yield significantly positive $\Delta\Phi$ values due to high hydrogen content detected by the neutron log. An initial threshold of $\Delta\Phi \geq 0.25$ was applied to classify shale intervals, although this value requires calibration against local geological conditions (Fertl & Chilingarian, 1987).

c. Gamma Ray (GR)

Shale lithologies generally exhibit high GR values due to elevated concentrations of radioactive minerals (K, U, Th). To minimize the effect of absolute measurement bias, the 70th percentile (P70) was applied as a relative cutoff. Intervals with $GR \geq P70$ were designated as shale candidates. This adaptive approach allows shale identification to be tailored to the characteristics of each individual well (Rider & Kennedy, 2011). The subset of shale intervals identified through this multi-parameter shale-picking process was subsequently used as the foundation for fitting the NCT. This ensures that the normal compaction curve accurately represents a pure loading trend, unaffected by non-shale lithologies or diagenetic alterations, thereby improving the reliability of pore pressure predictions.

2.1 Normal Compaction Trend (NCT)

The Normal Compaction Trend (NCT) describes the relationship between sonic velocity and burial depth. It provides the baseline against which anomalies in shale compaction can be evaluated to identify overpressure. The general form of the compaction equation is expressed as:

$$V = DT_0 * e^{-k \cdot z} + DT_\infty * (1 - e^{-k \cdot z}) \dots\dots\dots(\text{eq 1})$$

Where:

- V: sonic velocity (ft/s or m/s)
- DT_0 : velocity near the surface
- DT_∞ : asymptotic velocity at maximum shale compaction
- k: compaction gradient
- z: depth

The constants V_0 and k were derived from regression of sonic data within intervals of normally compacted shale, ensuring that the NCT accurately represents shale burial under hydrostatic conditions.

2.2 Eaton’s Method

This is an open access article under the HYPERLINK "https://creativecommons.org/licenses/by/4.0/" [CC BY 4.0](https://creativecommons.org/licenses/by/4.0/) license. Copyright ©2025 by Author. Published by Universitas Kristen Indonesia

Pore pressure was first estimated using the Eaton method (1975), which is widely applied for detecting undercompaction-related overpressure. The governing equation is:

$$P_p = S_v - (S_v - P_h) \left(\frac{\Delta t_n}{\Delta t} \right)^n \dots \dots \dots (\text{eq 3})$$

Where:

- P_p : pore pressure (psi)
- S_v : vertical stress (psi)
- P_h : hydrostatic pressure (psi)
- Δt_n : measured transit time ($\mu\text{s}/\text{ft}$)
- Δt : transit time for normally compacted shale ($\mu\text{s}/\text{ft}$)
- n : empirical exponent, typically between 3.0–4.0 (this study applied $n = 4.7$ for sonic logs)

$$S_v = \int_0^z \rho(z), g, dz \dots \dots \dots (\text{eq 4})$$

Where:

- $\rho(z)$ = bulk density (g/cc or kg/m^3),
- g = gravitasi ($9,81 \text{ m}/\text{s}^2$),
- z = depth (m or ft).

2.3 Bowers Velocity Model

The Bowers model (1995) extends pressure prediction beyond undercompaction, incorporating unloading effects. The model can be expressed as:

$$P_p = P_h + \left(\frac{\{V_n\}}{\{V\}} \right)^* (S_v - P_h) \dots \dots \dots (\text{eq 5})$$

Alternatively, the velocity–effective stress relationship can be written as:

$$V = V_0 + A(\sigma')^B \dots \dots \dots (\text{eq 6})$$

Where:

- V : sonic velocity (m/s)
- V_0 : reference velocity at zero effective stress (m/s)
- σ' : effective stress (psi)

A, B: empirical constants calibrated from well data

2.4 Minimum Effective Stress (Fracture Gradient)

The minimum horizontal stress (σ_{hmin}), representing the fracture gradient, was estimated using elasticity theory:

$$\sigma_{hmin} = \frac{\nu}{\{1-\nu\}(\sigma_v - P_p)} + P_p \dots \dots \dots (eq 7)$$

Where:

- σ_{hmin} : minimum effective stress (psi)
- ν : Poisson's ratio (0.25–0.30 for shale)
- σ_v : vertical stress (psi)
- P_p : pore pressure (psi)

3. Result and Discussion

The shale-picking process in well Penobscot B-41 successfully identified pure shale intervals, forming the basis for constructing the NCT and subsequent pore pressure estimation. Deviations between measured sonic transit time (DT) and the NCT became evident at depths of approximately 8,300–8,500 ft TVD, where DT values increased significantly compared to NCT predictions (Figure 4). This anomaly indicates the onset of overpressure, driven by incomplete compaction. The interpretation was corroborated by the absence of corresponding density reduction, suggesting that undercompaction was the dominant mechanism. The deviation intensified between ~9,000–9,200 ft TVD, forming a reversal zone. Here, the sonic response displayed evidence of unloading, as velocities decreased despite continued shale compaction. This observation highlights the coexistence of multiple overpressure mechanisms within the basin. The derived asymptotic transit time ($DT_{\infty} = 48 \mu\text{s}/\text{ft}$) confirmed that shales at this depth had reached maximum compaction, reinforcing the conclusion that deviations beyond this point represent true overpressure.

The calculated vertical stress gradient ($S_v = 1.018 \text{ psi}/\text{ft}$) aligns with values typical of clastic basins, indicating no significant density anomalies. Therefore, overpressure development is primarily attributed to loading–unloading processes rather than abnormal lithological variations. Eaton's method identified the first deviation at ~8,376 ft TVD, marking the top of overpressure. The Eaton-derived pore pressure curve exhibited a progressive increase with depth, reflecting the gradual buildup of excess pressure. The chosen exponent ($n = 4.70$) produced results more sensitive

to sonic deviations than the standard range (3–4), making the Eaton curve suitable as the lower bound estimate of pore pressure.

In contrast, calibration of the Bowers model ($V_0 = 5750$ ft/s, $A = 190$, $B = 0.43$) yielded pore pressure predictions higher than Eaton's at depths below the reversal zone (~9,000–9,200 ft TVD). This indicates significant unloading, manifested by reduced P-wave velocity relative to the loading curve, likely caused by fluid expulsion or smectite–illite transformation. Operationally, the Bowers curve is considered the upper bound estimate, providing a conservative design for drilling safety.

Fracture gradient analysis revealed that shallow intervals (< 8,000 ft TVD) remained stable with relatively high minimum effective stress (σ_{hmin}) values. However, beginning at 8,300–8,500 ft TVD (the top of overpressure), minimum effective stress (σ_{hmin}) decreased, narrowing the mud weight window. The most critical condition occurred at ~9,000–9,200 ft TVD, where unloading caused minimum effective stress (σ_{hmin}) to approach pore pressure, leaving a minimal drilling margin. This necessitates casing placement above the unloading interval and careful selection of mud weight between the Eaton and Bowers bounds to mitigate risks of influx or lost circulation.

4. Conclusion and Recommendation

4.1. Conclusion

The results of this study demonstrate that the integration of Eaton's method and the Bowers velocity model provides a more holistic understanding of pore pressure and stress distribution in the Penobscot Field. Eaton's method establishes a conservative baseline for detecting overpressure associated with undercompaction, thereby serving as the lower-bound reference for safe drilling. In contrast, the Bowers model captures the effects of unloading phenomena, which cannot be adequately explained by Eaton's formulation alone. This methodological integration ensures that both primary overpressure mechanisms are addressed, significantly improving the reliability of geopressure prediction. A critical finding of this research is the identification of the top of overpressure at approximately 8,376 ft TVD, which marks the onset of significant deviation from the normal compaction trend. Furthermore, a reversal zone was clearly observed at depths between 9,000–9,200 ft TVD. This interval is characterized by velocity reductions inconsistent with normal burial compaction, reflecting secondary processes such as fluid migration or mineral transformations. The recognition of these pressure transitions is essential, as they delineate the stratigraphic intervals most vulnerable to wellbore instability.

The comparative analysis revealed that pore pressure estimates derived from the Bowers model consistently exceed those of the Eaton method within unloading intervals. This discrepancy underscores the operational importance of using Bowers' predictions as an upper-bound estimate in order to safeguard against unexpected high-pressure zones. In drilling practice, reliance solely on Eaton's lower-bound values could underestimate true pore pressure magnitudes, thereby increasing the risk of well control incidents.

The unloading zone, in particular, was identified as the most critical interval for drilling operations. In this depth range, the effective stress approaches pore pressure, resulting in a narrow mud weight window. Under such conditions, even minor inaccuracies in mud weight selection

could trigger severe operational risks, including kicks, lost circulation, or blowouts. This emphasizes the necessity of adopting a dual-model framework in which both Eaton and Bowers are applied to define operational safety margins.

From an engineering perspective, the study concludes that safe drilling in the Penobscot B-41 well requires careful casing design and mud weight management. Casing seats should be positioned above the unloading interval to isolate unstable formations, while mud weights must be optimized between the Eaton-derived lower bound and the Bowers-derived upper bound. Adherence to this approach will enhance drilling safety, reduce non-productive time, and mitigate the risk of catastrophic well control events.

4.2. Recommendation

Based on the findings of this study, several recommendations are proposed to strengthen future research and operational practices in the Penobscot Field.

First, a multidisciplinary integration of methods is strongly recommended for future pore pressure and fracture gradient prediction efforts. While Eaton's and Bowers' methods have proven effective in capturing undercompaction and unloading mechanisms, reliance on well-log-based approaches alone may limit predictive accuracy, particularly in areas with complex stratigraphy or lateral variations. The incorporation of seismic velocity analysis, calibrated against well data, can provide a broader spatial perspective and significantly improve the robustness of geopressure models. Such integration would also allow for cross-validation of results, thereby reducing uncertainty and enhancing the predictive reliability of overpressure regimes.

Second, the application of 3D geopressure modeling is advised to account for the lateral heterogeneity observed across the Penobscot Field. Overpressure systems are inherently variable, and extrapolation from a single well can be insufficient for regional-scale drilling and development planning. By utilizing three-dimensional seismic velocity data, a more comprehensive and spatially consistent assessment of pore pressure distribution can be achieved. This approach will not only refine local well design but also support broader exploration strategies and field development scenarios, minimizing the risks associated with unexpected pressure anomalies in adjacent areas.

Finally, special emphasis must be placed on drilling planning and wellbore stability management, particularly in relation to the unloading interval identified between ~9,000–9,200 ft TVD. This zone represents the most critical operational challenge due to its narrow mud weight window, where pore pressure approaches the fracture gradient. It is therefore recommended that casing seats be strategically positioned above this interval to isolate unstable formations and mitigate the risks of kicks and lost circulation. Moreover, the design of the mud weight program should carefully balance between the Eaton-derived lower bound and the Bowers-derived upper bound, ensuring both well control and formation integrity. By adopting these measures, drilling operations in the Penobscot Field can be conducted with greater safety, efficiency, and long-term reliability.

5. Acknowledgments

Thank you to the parties who have contributed, namely supervisors, colleagues, supporting institutions, funders, or research participants.

6. References

- Athy, L. F. (1930). Density, porosity, and compaction of sedimentary rocks. *AAPG Bulletin*, 14(1), 1–24.
- Bachu, S., & Underschlutz, J. R. (1995). Large-scale underpressuring in the Western Canada Sedimentary Basin. *AAPG Bulletin*, 79(4), 551–572.
- Bowers, G. L. (1995). Pore pressure estimation from velocity data: Accounting for overpressure mechanisms besides undercompaction. *SPE Drilling & Completion*, 10(2), 89–95.
- Bruce, C. H. (1984). Smectite dehydration—its relation to structural development and hydrocarbon accumulation in Northern Gulf of Mexico Basin. *AAPG Bulletin*, 68(5), 673–683.
- Dutta, N. C. (2002). Geopressure prediction using seismic data: Current status and the road ahead. *Geophysics*, 67(6), 2012–2041.
- Eaton, B. A. (1975). The equation for geopressure prediction from well logs. SPE Paper 5544. Society of Petroleum Engineers.
- Fertl, W. H., & Chilingarian, G. V. (1987). *Abnormal formation pressures*. Amsterdam: Elsevier.
- Horsrud, P. (2001). Estimating mechanical properties of shale from empirical correlations. *SPE Drilling & Completion*, 16(2), 68–73.
- Jansa, L. F., & Wade, J. A. (1975). Geology of the continental margin off Nova Scotia and Newfoundland. In *Canadian Society of Petroleum Geologists Memoir* (Vol. 4, pp. 79–102).
- Kidston, A., Brown, D. E., Smith, B. M., & Althelm, B. (2002). Geology of the Sable Subbasin offshore Nova Scotia. *Canada-Nova Scotia Offshore Petroleum Board Reports*.
- Law, B. E., & Spencer, C. W. (1998). *Abnormal pressure in hydrocarbon environments*. U.S. Geological Survey Bulletin 2164. Denver, CO: USGS.
- Osborne, M. J., & Swarbrick, R. E. (1997). Mechanisms for generating overpressure in sedimentary basins: A re-evaluation. *AAPG Bulletin*, 81(6), 1023–1041.
- Rider, M., & Kennedy, M. (2011). *The geological interpretation of well logs* (3rd ed.). Rider-French Consulting Ltd.
- Sayers, C. M. (2010). Geophysics under stress: Geomechanical applications of seismic and borehole acoustic waves. *The Leading Edge*, 29(12), 1494–1502.
- Swarbrick, R. E., & Osborne, M. J. (1998). Mechanisms that generate abnormal pressures: An overview. In B. E. Law, G. F. Ulmishek, & V. I. Slavin (Eds.), *Abnormal pressures in hydrocarbon environments* (pp. 13–34). AAPG Memoir 70.
- Swarbrick, R. E., Osborne, M. J., & Yardley, G. S. (2002). Overpressure in petroleum exploration. *Geological Society, London, Special Publications*, 207(1), 1–12.
- Terzaghi, K. (1943). *Theoretical soil mechanics*. New York: Wiley.
- Wade, J. A., & MacLean, B. C. (1990). *The geology of the southeastern margin of Canada*. Geological Survey of Canada, Geology of Canada Series No. 2.